ISSN 0915-633X

NATIONAL INSTITUTE FOR FUSION SCIENCE

Phase Diagram of Structure of Radial Electric Field in Helical Plasmas

S. Toda and K. Itoh

(Received - Dec. 21, 2001)

NIFS-722 Jan. 2002

RESEARCH REPORT
NIFS Series

TOKI, JAPAN

Phase diagram of structure of radial electric field in helical plasmas

S. Toda and K. Itoh

National Institute for Fusion Science,

322-6 Oroshi, Toki, Gifu 509-5292, Japan

(Dated: January 8, 2002)

Abstract

A set of transport equations in toroidal helical plasmas is analyzed, including the bifurcation of the radial electric field. Multiple solutions of E_r for the ambipolar condition induces domains of different electric polarities. A structure of the domain interface is analyzed and a phase diagram is obtained in the space of the external control parameters. The region of the reduction of the anomalous transport is identified.

Keywords: radial electric field, neoclassical transport,anomalous transport, phase diagram,transition property

The internal transport barrier (ITB) has been found in electron cyclotron resonance heating (ECRH) plasma in Compact Helical System (CHS) and the steep gradient in the profile of the radial electric field has been obtained in the inner region [1]. The observation of the internal transport barrier is also confirmed by Wendelstein7-AS (W7-AS) stellarator [2] and the problem of the ITB in helical systems provides a key to understand the essential nonlinear property of toroidal plasmas. There are two important issues. The first is the spatial formation of the radial electric field, which is associated with the steep gradient of the radial electric field E_r. The generation of the electric field in helical systems could be investigated more quantitatively because the neoclassical transport is found to play the dominant role in generating the radial electric field (See articles, [3, 4] and reviews, *e.g.*, [5–7]). Study on the localized structure of the gradient of E_r has been performed in helical plasmas [8]. The second is the study of the turbulent transport and the neoclassical energy transport so as to understand the formation of the internal transport barrier. The self-consistent transport study has been done in which both the electric field bifurcation and suppression of the anomalous transport are included in order to analyze the structure of the electric field quantitatively [9]. The transport model (e.g. [10]) for anomalous diffusivities was adopted in CHS typical machine parameters. In tokamaks, structure and dynamics of the transport barrier have been also studied by using an analytical model [11, 12].

In this article, types of the structure of the radial electric field are studied and a phase diagram of a bifurcation of E_r profile is investigated. When the multiple solutions of E_r of the ambipolar condition causes the steep spatial gradient of E_r. Due to this steep gradient of E_r, the reduction of the anomalous transport is obtained. In this case, we call the transition hard-typed. When the transition occurs without multiple ambipolar E_r, the steep gradient of E_r is not obtained and the spatial change of E_r becomes smooth. We call this transition soft-typed. A phase diagram of the structure of the radial electric field in the space of external control parameters is obtained. This is a typical example of the non-equilibrium phase diagram for open systems. The change of the transition types is studied in a phase diagram.

The cylindrical coordinate is used and r-axis is taken in the radial cylindrical plasma in this article. The region $0 \leq r \leq a$ is considered, where a is the minor radius. The total particle flux Γ^t is written as $\Gamma^t = \Gamma^{na} - D_a n'$, where D_a is the anomalous particle diffusivity and the prime denotes the derivative with respect to the radial direction. Here, Γ^{na} is the radial neoclassical flux associated with helical-ripple trapped particle [13]. The total heat

flux Q_j^t of the species j is written as $Q_j^t = Q_j^{na} - n\chi_a T_j'$. where χ_a is the anomalous heat diffusivity and Q_j^{na} is the energy flux by the ripple transport, respectively. The theoretical model for the anomalous heat conductivity will be explained later. The neoclassical diffusion coefficient for the electric field is shown in ref. [14] and is denoted by D_{Ea}. The one-dimensional transport equations used here are same as those shown in ref. [8]. Throughout this article, the heating source of electrons and ions are set to be proportional to the relation $exp(-(r/(0.2a))^2)$, which corresponds to the central heating experimentally, *e.g.*, the ECRH.

We fix the boundary condition at the center of the plasma (r=0) such that $n' = T_e' = T_i' = E_r = 0$. For the radial electric field E_r, the boundary condition at the edge (r=a) is chosen as $\sum_j Z_j \Gamma_j = 0$. This simplification is employed because the electric field bifurcation in the core plasma is the main subject of this study. The boundary conditions at the edge (r=a) with respect to the density are those expected in CHS: $-n/n' = 0.05\text{m}$, $-T_e/T_e' = -T_i/T_i' = 0.02\text{m}$. The machine parameters are similar to those of CHS device, such as $R = 1\text{m}$, $a = 0.2\text{m}$, the toroidal magnetic field $B = 1\text{T}$, toroidal mode number $m = 8$ and the poloidal mode number $\ell = 2$. We set the safety factor and the helical ripple coefficient as $q = 3.3 - 3.8(r/a)^2 + 1.5(r/a)^4$ and $\varepsilon_h = 0.231(r/a)^2 + 0.00231(r/a)^4$, respectively [1]. The particle source S_n is set to be $S_n = S_0 \exp((r-a)/L_0)$, where L_0 is set to be $0.01(m)$ and is considered to include the ionization effect near the edge. The value of S_0 is strongly influenced by the particle confinement time. The value for the anomalous diffusivities of the particle is chosen $D_a = 10\text{m}^2\text{s}^{-1}$. This value is set to be constant spatially and temporally.

In this study, we adopt the model for the anomalous heat conductivity based on the theory of the self-sustained turbulence due to the ballooning mode and the interchange mode, both driven by the current difffusivity [10, 15] as a candidate. The reduction of the anomalous transport due to the inhomogeneous radial electric field was theoretically reported in the toroidal helical system. (The validity of this model for heliotron/torsatron plasmas has not yet completely been investigated by comparing with experimental results. This model predicted a trend of χ_a that χ_a can reduce as the magnetic axis is shifted inward in the Large Helical Device (LHD) or the CHS. This has the relevance for the experimental observation [16].) The anomalous transport coefficient for the temperatures is given as $\chi_a = \chi_0/(1 + G\omega_{E1}^2)$, where $\chi_0 = F(s,\alpha)\alpha^{\frac{3}{2}} c^2 v_A/(\omega_{pe}^2 qR)$. The factor $F(s,\alpha)$ is the function of the magnetic shear s and the normalized pressure gradient α, defined by $s = rq'/q$ and $\alpha = -q^2 R\beta'$. For the ballooning mode turbulence for the system with a magnetic well, we employ the anomalous thermal conductivity $\chi_{a,BM}$. The details about

the coefficients $F(s,\alpha)$, G, and the factor ω_{E_1}, which stands for the effect of the electric field shear, are given in ref. [15] in the ballooning mode turbulence. In the case of the interchange mode turbulence for the system of the magnetic hill [10], we adopt the the anomalous thermal conductivity $\chi_{a,IM}$. The details about F, G, and the factor ω_{E_1} in the case of the interchange mode were given in ref. [10]. The greater one of the two diffusivities is adopted, $\chi_a = \max(\chi_{a,BM}, \chi_{a,IM})$. The approximation $D_{Ea} = \chi_a$ is employed, where the validity of this approximation is discussed in ref. [17].

We use the typical machine parameters of CHS. The stationary solution of the radial electric field is obtained. In a parameter region, the transition of the radial electric field is found. When the value of the obtained temperature or the density changes, the profile of the stationary electric field takes three types of roots. The parameter region of the three root patterns of the stationary electric field is shown in the $\bar{n} - \bar{T}_e/\bar{T}_i$ plane in Fig. 1, where the bar shows the line-averaged quantity. At first, all stationary electric fields in the radial points takes the electron root ($E_r > 0$) in the region labelled e. Secondly, when the density increases, the stationary electric field in the core plasma takes the electron root and the electric field in the outer plasma takes the ion root ($E_r < 0$) in the region labelled $e - i$. Furthermore, in this case, the type of the transition is classified to the soft or hard one. We call the transition between the multiple solutions for the ambipolar condition the hard one. We set the transition point $\rho = \rho_T$, where $\rho = r/a$. The electron root for $\rho < \rho_T$ is sharply connected to the ion root for $\rho > \rho_T$ with a thin layer between them. The absolute value of the gradient for the electric field at the transition point is about $1 \times 10^6 \mathrm{V/m}^2$ and this is enough large to suppress the anomalous transport considered here. Multiple solutions which hold the local ambipolar condition is needed for the spatial transition to take place rapidly. The multiple solutions are obtained in the hatched region: $\bar{T}_e/\bar{T}_i \approx 2$ and $\bar{n} = (2-7) \times 10^{18}\mathrm{m}^{-3}$. In this hatched region, the transport barrier is obtained for the both channels of the sum of the neoclassical transport and the anomalous transport, although it is not very clear in both the electron and ion temperature profiles. The reduction of χ_a is obtained due to the strong gradient of the electric field at the transition point. The profiles of the neoclassical diffusivities of electrons χ_e^{NEO} and ions χ_i^{NEO} are also obtained. In this case of the spatial transition, the electric field goes across zero at $\rho \approx \rho_T$. Therefore, the neoclassical diffusivities have a peak near the surface where the relation $E_r \approx 0$, because they depend on the value of E_r itself. The total suppression is found to exist but is small compared with that of the anomalous diffusivity. On the other hand, the transition in

which one solution for the ambipolar condition exists is called the soft one. In the region labelled $e-i$ in which the electron root and the ion root co-exist outside the hatched region, the spatial slow transition occurs without the multiple solutions. In this case of the soft transition, there is no reduction of the anomalous transport due to the gradient of the radial electric field. When the value of the density becomes much larger ($\bar{n} \approx 10^{20}\mathrm{m}^{-3}$), all radial stationary electric fields take the ion root in the region labelled i.

Figure 1 is a phase diagram for the structural formation of plasmas. Changes of properties across the phase boundaries attract attentions. When the control parameters move across the boundary between the regions i and $e-i$, the domain of the positive electric field (electron root) appears ($i \to e-i$) or disappears ($e-i \to i$) at the center of plasmas. At the boundary between the regions $e-i$ and e, the domain of the negative electric field (ion root) disappears ($e-i \to e$) or appears ($e \to e-i$) at the plasma boundary. These two phase boundaries are related to the radial location of the domain interface of E_r.

The phase boundary between the hard transition and soft transition is characterized by the steepness of the radial gradient of E_r and the transition property across the phase boundary is studied. The maximum value of $|dE_r/dr|$ in the radial direction is examined along the arrow in the region labelled $e-i$ in Fig.1, in order to study the qualitative difference between the hard and soft transitions. The gradient of the radial electric field takes the maximum value around the point in which the transition occurs. Figure 2 shows the dependence of the maximum value of $|dE_r/dr|$ on the change of the averaged density $\bar{n}$. The dashed line represents the boundary whether the multiple solutions for the ambipolar E_r exist or not. In the case of the hard transition ($\bar{n} \approx 3 \times 10^{18}\mathrm{m}^{-3}$), the value of the maximum value becomes larger about $5 \times 10^5\mathrm{V/m}^2$, which induces the reduction of the anomalous heat conductivity. The gradient of the radial electric field becomes weak in the region $\bar{n} \approx 1 \times 10^{19}\mathrm{m}^{-3}$, where the soft transition in the E_r profile is found. In this region, the gradient of the radial electric field is not enough strong to suppress the anomalous heat conductivity considered here. The value of the gradient of the radial electric electric field does not change very much when the value of the density changes in the region of the soft transition, being saturated to be the order of $T_e/(ea^2)$. On the other hand, the value of $|dE_r/dr|$ becomes large when the value of the averaged density becomes smaller. The enhancement of $|dE_r/dr|$ is due to the narrow region across which the electric field changes from the positive value to the negative value (Fig. 3). This narrow layer is determined by the competition between the thickness of nonlinearity in $\Gamma(E_r)$. The suppression of the

turbulence decreases D_{Ea} so as to reduce the thickness. Thus the large value of $|dE_r/dr|$ self-sustains. The change of the maximum of the electric field gradient occurs with a finite difference of the plasma density after the transition type becomes from soft to hard. This is because the contribution of the radial derivative for D_{E_a} can not be neglected when the diffusivity D_{E_a} includes the effect of the profile of the plasma quantities. The example of the hard and soft transitions of the radial electric field is shown in Fig. 3. The solid line shows the case of the hard transition between the multiple ambipolar solutions of E_r. The hard transition occurs with the rapid spatial change of E_r from the positive E_r to the negative E_r. The dotted line represents the profile of the radial electric field in which the soft transition (without multiple ambipolar E_r) takes place. (Note that the bifurcation of E_r near the magnetic axis is due to the model of χ_a which becomes smaller if the pressure gradient vanishes [10]. This point is not the subject of this article.)

In summary, the structure of the radial electric field in helical plasmas is theoretically studied. The different types of the E_r structure are examined and a phase diagram is obtained on $\bar{n} - \bar{T}_e/\bar{T}_i$ plane. The hard transition of the E_r structure between the multiple ambipolar E_r is obtained in this study of $T_e/T_i \approx 2$. In the region of the hard transition, the absolute value of the electric field gradient takes the large value: $|dE_r/dr| \approx 5 \times 10^5 \mathrm{V/m}^2$, which is enough to suppress the anomalous transport studied here. When $T_e/T_i \approx 3$ and the value of the density takes about $1 \times 10^{19} \mathrm{m}^{-3}$, the transition type is found to become soft (without multiple ambipolar E_r). The condition for the suppression of the anomalous diffusivities is suggested to be rather high T_i in addition to the low density and high T_e Furthermore, the change of the transition types is studied in the phase diagram of the external control parameters. To examine the transition types, we show the dependence of $|dE_r/dr|$ on the line-averaged density. It should be noted that the maximum value of $|dE_r/dr|$ and the width of the transition layer at $\rho = \rho_T$ give an experimental test for the transport model employed here. The obtained value of the maximum of $|dE_r/dr|$ is in the range of the experimental observation. The comparison of the transition layer thickness has given an experimental estimate of $D_{Ea} \approx 6\mathrm{m}^2/\mathrm{s}$ and the condition of the confinement improvement. This theoretical model used here is not rejected by these experimental results.

Finally, in CHS device, the spatial transition from the larger positive E_r to the smaller positive E_r is observed [1]. Such a spatial transition does not induce a local peak of χ_j^{NEO}, and should be searched for in simulations. This is left for the future study.

Authors would like to acknowledge Prof. S. -I. Itoh, Prof. A. Fukuyama and Dr. M. Yagi

for illuminating discussion and the suggestion for the analysis. In particular, one of the authors (ST) thanks Prof. A. Fukuyama for the helpful suggestions in numerical methods. Discussions about the related experimental results with Dr. A. Fujisawa, Prof. K. Ida and H. Sanuki are also acknowledged. This work is partially supported by the collaboration programs of National Institute for Fusion Science (NIFS) and Research Institute for Applied Mechanics (RIAM) in Kyushu University, and Grant-in-Aid for Scientific Research on Ministry of Education, Culture, Sports, Science and Technology of Japan.

---

[1] A. Fujisawa *et al.*, Phys. Plasmas **7,** 4152 (2000).

[2] U. Stroth *et al.*, Phys. Rev. Lett. **86,** 5910 (2001).

[3] H. Sanuki *et al.*, J. Phys. Soc. Jpn. **60,** 3698 (1991).

[4] H. Maaßberg *et al.*, Phys. Plasmas **7,** 295 (2000).

[5] L. M. Kovriznykh, Nucl. Fusion **24,** 851 (1984).

[6] K. Ida, Plasma Phys. Control. Fusion **40,** 1429 (1988).

[7] K. Itoh, S. -I. Itoh, and A. Fukuyama, Transport and Structural Formation in Plasmas (London, UK: Institute of Physics Publishing, 1999) ch 12.

[8] S. Toda and K. Itoh, Plasma Phys. Control. Fusion **43,** 629 (2001).

[9] S. Toda and K. Itoh, *in Proceedings of the 28th EPS Conf. on Control. Fusion and Plasma Phys. (18-22 June 2001, Funchal, Portugal)* P4.055 (2001).

[10] K. Itoh *et al.*, Plasma Phys. Control. Fusion **34,** 123 (1994).

[11] P. H. Diamond, V. B. Lebedev, D. E. Newman, and B. A. Carreras, Phys. Plasmas **2,** 3685 (1995).

[12] P. H. Diamond *et al.*, Phys. Rev. Lett. **78,** 1472 (1997).

[13] K. C. Shaing, Phys. Fluids **27,** 1567 (1984).

[14] D. E. Hastings, Phys. Fluids **28,** 334 (1985).

[15] K. Itoh *et al.*, Plasma Phys. Control. Fusion **36,** 279 (1994).

[16] H. Yamada *et al*, Plasma Phys. Control. Fusion. **43,** A55 (2001).

[17] K. Itoh *et al.*, J. Phys. Soc. Jpn. **62,** 4269 (1993).

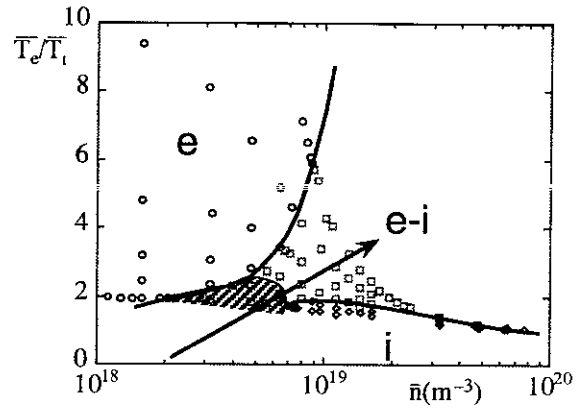

FIG. 1: Three patterns of the ambipolar solutions of E_r are clarified in the $\bar{n} - \bar{T}_e/\bar{T}_e$ plane. In the hatched region, multiple solutions of ambipolar E_r are obtained, which are needed to obtain the spatial rapid change of the stationary profile for E_r.

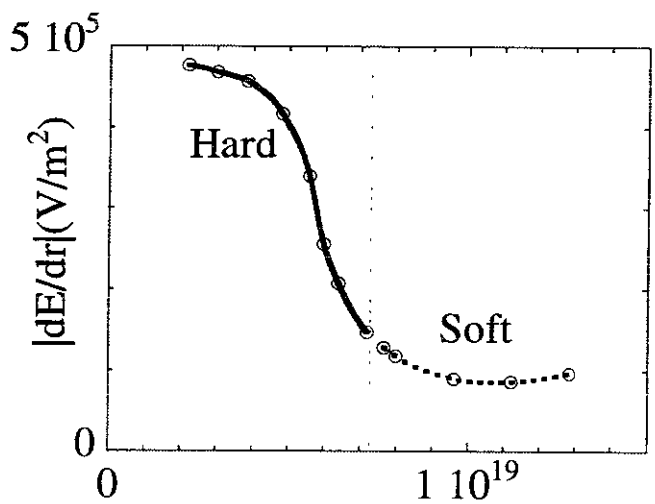

FIG. 2: The dependence of the maximum of $|dE_r/dr|$ on the averaged density. The dashed line shows the boundary between the hard and soft transition.

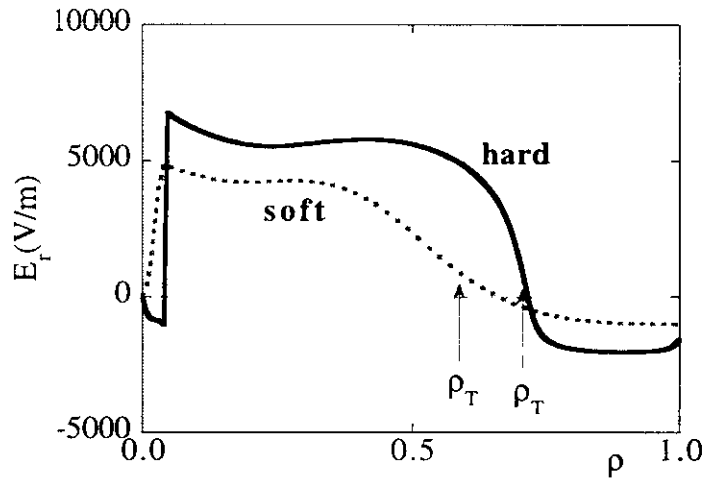

FIG. 3: The example of the hard (solid line) and soft (dotted line) transition in the profile of the radial electric field. Gradient of E_r across the transition surface ρ_T is much smaller for the case of the soft transition than the case of the hard transition.

Recent Issues of NIFS Series

NIFS 697 M Yokoyama, K Itoh, S Okamura, K Matsuoka, S -I Itoh,
Maximum J Capability in a Quasi-Axisymmetric Stellarator May 2001

NIFS-698 S-I Itoh and K Itoh,
Transition in Multiple scale lengths Turbulence in Plasmas May 2001

NIFS 699 K Ohi, H Naitou, Y Tauchi, O Fukumasa,
Bifurcation in Asymmetric Plasma Divided by a Magnetic Filter May 2001

NIFS-700 H Miura, T Hayashi and T Sato,
Nonlinear Simulation of Resistive Ballooning Modes in Large Helical Device June 2001

NIFS 701 G Kawahara and S Kida
A Periodic Motion Embedded in Plane Couette Turbulence June 2001

NIFS 702 K Ohkubo
Hybrid Modes in a Square Corrugated Waveguide June 2001

NIFS-703 S -I Itoh and K Itoh,
Statistical Theory and Transition in Multiple-scale-lengths Turbulence in Plasmas June 2001

NIFS-704 S Toda and K Itoh,
Theoretical Study of Structure of Electric Field in Helical Toroidal Plasmas June 2001

NIFS-705 K Itoh and S-I Itoh,
Geometry Changes Transient Transport in Plasmas June 2001

NIFS-706 M Tanaka and A Yu Grosberg
Electrophoresis of Charge Inverted Macroion Complex Molecular Dynamics Study July 2001

NIFS-707 T-H Watanave, H Sugama and T Sato
A Nondissipative Simulation Method for the Drift Kinetic Equation, July 2001

NIFS 708 N Ishihara and S Kida,
Dynamo Mechanism in a Rotating Spherical Shell Competition between Magnetic Field and Convection Vortices July 2001

NIFS-709 LHD Experimental Group,
Contributions to 28th European Physical Society Conference on Controlled Fusion and Plasma Physics (Madeira Tecnopolo, Funchal, Portugal 18-22 June 2001) from LHD Experiment July 2001

NIFS-710 V Yu Sergeev, R K Janev, M J Rakovic, S Zou, N Tamura, K V Khlopenkov and S Sudo
Optimization of the Visible CXRS Measurements of TESPEL Diagnostics in LHD, Aug 2001

NIFS-711 M Bacal, M Nishiura, M Sasao, M Wada, M Hamabe, H Yamaoka,
Effect of Argon Additive in Negative Hydrogen Ion Sources, Aug 2001

NIFS-712 K. Saito, R Kumazawa, T Mutoh, T Seki, T Watari, T Yamamoto, Y Torii, N Takeuchi C Zhang, Y Zhao, A Fukuyama, F Shimpo, G Nomura, M Yokota, A Kato, M Sasao, M Isobe, A V. Krasilnikov, T Ozaki M Osakabe, K Narihara, Y Nagayama, S Inagaki, K Itoh, T Ido, S Morita, K Ohkubo, M Sato, S Kubo, T Shimozuma, H Idei, Y Yoshimura, T Notake, O Kaneko, Y Takeiri, Y Oka, K Tsumori, K Ikeda, A Komori, H Yamada, H Funaba, K Y Watanabe, S Sakakibara, R Sakamoto, J Miyazawa, K Tanaka, B J Peterson, N Ashikawa S Murakami, T Minami, M Shoji, S Ohdachi S Yamamoto H Suzuki, K Kawahata, M Emoto, H Nakanishi, N Inoue, N Ohyabu Y Nakamura, S Masuzaki, S Muto, K Sato, T Morisaki M Yokoyama, T Watanabe, M Goto, I Yamada, K Ida, T Tokuzawa, N Noda K Toi, S Yamaguchi, K Akaishi A Sagara, K Nishimura, K Yamazaki, S Sudo Y Hamada, O. Motojima, M Fujiwara,
A Study of High-Energy Ions Produced by ICRF Heating in LHD Sep 2001

NIFS-713 Y Matsumoto S -I Oikawa and T Watanabe,
Field Line and Particle Orbit Analysis in the Periphery of the Large Helical Device, Sep 2001

NIFS-714 S Toda, M Kawasaki, N Kasuya, K Itoh, Y Takase, A Furuya, M Yagi and S -I Itoh,
Contributions to the 8th IAEA Technical Committee Meeting on H-Mode Physics and Transport Barriers (5-7 September 2001, Toki, Japan) Oct 2001

NIFS-715 A Maluckov N Nakajima M Okamoto, S Murakami and R Kanno
Statistical Properties of the Particle Radial Diffusion in a Radially Bounded Irregular Magnetic Field Oct 2001

NIFS-716 Boris V Kuteev
Kinetic Depletion Model for Pellet Ablation, Nov 2001

NIFS-717 Boris V Kuteev, Lev D. Tsendin,
Analytical Model of Neutral Gas Shielding for Hydrogen Pellet Ablation Nov 2001

NIFS-718 Boris V Kuteev,
Interaction of Cover and Target with Xenon Gas in the IFE-Reaction Chamber Nov 2001

NIFS-719 A Yoshizawa, N Yokoi, S -I Itoh and K Itoh,
Mean-Field Theory and Self-Consistent Dynamo Modeling Dec 2001

NIFS 720 V N Tsytovich and K Watanabe,
Universal Instability of Dust Ion-Sound Waves and Dust-Acoustic Waves Jan 2002

NIFS-721 V N Tsytovich
Collective Plasma Corrections to Thermonuclear Reactions Rates in Dense Plasmas Jan 2002

NIFS-722 S Toda and K Itoh
Phase Diagram of Structure of Radial Electric Field in Helical Plasmas Jan 2002